Structural characterization of oxidized titanium surfaces

Jobin, Marc; Taborelli, Mauro; Descouts, Pierre

How to cite

JOBIN, Marc, TABORELLI, Mauro, DESCOUTS, Pierre. Structural characterization of oxidized titanium surfaces. In: Journal of Applied Physics, 1995, vol. 77, n° 10, p. 5149–5155. doi: 10.1063/1.359259

This publication URL: https://archive-ouverte.unige.ch/unige:98964
Publication DOI: 10.1063/1.359259

Structural characterization of oxidized titanium surfaces

M. Jobin, M. Taborelli, and P. Descouts

Citation: Journal of Applied Physics **77**, 5149 (1995);
View online: https://doi.org/10.1063/1.359259
View Table of Contents: http://aip.scitation.org/toc/jap/77/10
Published by the American Institute of Physics

Structural characterization of oxidized titanium surfaces

M. Jobin, M. Taborelli, and P. Descouts
Groupe de Physique Appliquée, Université de Genève, 20 rue de l'Ecole de Médecine, CH-1211 Genève 4, Switzerland

(Received 24 October 1994; accepted for publication 27 January 1995)

Oxidized titanium surfaces resulting from various processes have been structurally characterized by means of scanning force microscopy, x-ray photoemission spectroscopy (XPS), x-ray diffraction, and electron energy-loss spectroscopy (EELS) with losses in the 0–100 eV range. It has been found that the surface morphology has a granular structure for electropolished titanium and for titanium evaporated on mica at low substrate temperature (570 K), but changes to flat terraces for the films evaporated at higher temperature (770 K). Angular-dependent XPS has revealed the presence of a Ti_2O_3 suboxide at the Ti/TiO_2 interface for electropolished titanium. Dry oxidation has been performed at 770 and 970 K on both weakly and highly crystallized evaporated titanium films oriented along (0001). In the case of underlying crystallized metallic titanium, the resulting TiO_2 films are crystallized with the anatase (004) orientation for oxidation at 770 K and with rutile (200) orientation for oxidation at 970 K. EELS spectra interpreted in terms of the molecular orbitals of a $(TiO_6)^{8-}$ cluster show that the local octahedral environment of titanium atoms is preserved on native oxides, even if these oxides are not crystallized. © *1995 American Institute of Physics.*

I. INTRODUCTION

The surface properties of titanium dioxide (TiO_2) are extensively exploited in various industrial fields for three main reasons. First, the passivation of metallic titanium by its native oxide provides a very corrosion resistant material. In connection with favorable mechanical properties, this corrosion resistance is responsible for the great success in using titanium for orthopaedic implants.[1] Second, the high refractive index and low absorption coefficient of TiO_2 make this material very attractive as optical coating, especially in view of gradient index coatings.[2] Third, the photocatalytic activity of the TiO_2 surface has received much attention since its discovery[3] and has found practical applications, for example, in solar energy conversion.

A number of techniques have been used to produce thick films of titanium oxide including sputtering, chemical-vapor deposition (CVD), and anodic growth. Structural characterizations have been performed mainly by x-ray diffraction (XRD) and can be summarized as follows: for sputter-deposited films[4] the oxide is mainly amorphous before 570 K, the anatase structure is more predominant at substrate temperature in the range of 570–770 K,[5] while the rutile structure occurs for substrate temperatures above 870 K. Annealing of an amorphous TiO_2 film[6] leads to anatase transformation at 620 K and to rutile transformation at 870 K. Similar results hold for metal-organic CVD (MOCVD) films,[7] as well as for laser-annealed amorphous TiO_2 films. The anatase structure is observed at low laser power and a mixture of anatase and rutile is observed at higher power.[8] In most of these studies the substrate is not titanium and the thickness of the TiO_2 film is large compared to the one of native oxide on pure titanium.

In this report we are more concerned with the thin native oxide film (thickness of about 5 nm) which develops spontaneously when bulk titanium is exposed to air, oxygen, or water, or after a surface treatment such as electropolishing. The properties of this oxide are of particular interest in view of medical implants mentioned above, since the direct growth of the bone observed on titanium (therefore on the thin native oxide film) is not yet understood.[9] Since this phenomenon—named osseointegration—is clearly an interfacial problem, it is of interest to know the structural properties of such native oxides and to investigate in what extent we can improve them. As an example, we have investigated thermally grown oxide obtained through annealing of titanium films in oxygen atmosphere.

The main difficulty in the study of titanium native oxide films is that they cannot be cleaned in UHV with standard procedures; annealing leads to oxygen diffusion toward bulk, and sputter cleaning damages a large portion of its thickness. Therefore, all samples have been characterized immediately after preparation without any additional treatment or cleaning procedure. The hydrocarbon contamination did not prevent us from acquiring clear electron energy-loss spectroscopy (EELS) or x-ray photoemission spectroscopy (XPS) spectra, since the electron mean free path is much larger than the contamination layer.

II. SAMPLE PREPARATION

In this section we briefly describe the preparations of the various samples we have used. Mechanically polished and electropolished samples were prepared from bulk commercially pure (c.p.) Ti 99.6% platelets (from Goodfellow). This grade purity is often used for manufacturing orthopaedic titanium implants. Mechanical polishing was performed with SiC abrasive sheets up to grade 4000 [the grain size of SiC is about 5 μm, as determined by scanning electron microscopy (SEM)]. No incorporation of silicon was recorded by Auger spectroscopy. Subsequent electropolishing was performed in a commercial electrolyte (Struers A3) containing perchloric acid. The electropolishing parameters and the properties of such surfaces have been published elsewhere.[10]

Thick titanium films (150 nm) have been evaporated on freshly cleaved muscovite mica by means of an electron-

beam evaporator (Leybold ESV-2). The growth rate was 0.1 nm/s. The base pressure during evaporation was 5×10^{-7} mbar, but only traces of oxygen were found on Auger depth profiles. Indeed, the level of incorporated oxygen was not higher in the evaporated films than in the bulk Ti samples. As expected, evaporated titanium on mica results in a film oriented along the c axis[11] and its degree of crystallization depends strongly on the substrate temperature, as shown below.

The thermal oxides have been produced from these evaporated films. We have used a high-pressure furnace containing an Ar atmosphere at 1 kbar and 20 ppm O_2 at a controlled temperature (ranging from 500 to 1000 K). The temperature was held constant during the oxidation time, which was set to 1 h. The resulting oxides were not uniform in color which shows thickness variation of several nanometers.

Finally, we also used a TiO_2 (110)-rutile single crystal as a reference for the EELS studies. After several cycles of Ar^+ sputtering and thermal annealing, this single crystal produced a clear 1×1 low-energy electron-diffraction (LEED) pattern.

III. RESULTS

A. Scanning force microscopy

We have used a scanning force microscope (SFM) in air (Park Scientific Instrument BD-2) to measure the surface topography of the "as prepared" surfaces. All images presented here have been acquired in the repulsive dc mode since no damage was expected on such hard surfaces. We have used stiff V-shaped cantilevers with Si_3N_4 integrated pyramidal tips (the compliance is 0.35 N/m according to the supplier) in order to reduce the lever torsion due to friction, as seen by the very small difference in the line scan as the sample is moved back and forth. Nevertheless, tips break easily on titanium surfaces with resulting artifacts on the SFM images, and a large number of data have to be acquired with various tips before the real size of the structures can be confidently extracted.

Representative SFM images are shown in Fig. 1 for mechanically polished titanium [Fig. 1(a)], electropolished Ti [Fig. 1(b)], and evaporated Ti on mica at 570 K [Fig. 1(c)] and at 770 K [Fig. 1(d)]. As expected, mechanically polished samples are the roughest and the less homogeneous ones (the scan size is 5×5 μm^2) due to the presence of the polishing grooves. The smallest measured grooves are about 25 nm wide and 1.6 nm deep, which can be compared with the grain size of the finest abrasive sheet (5 μm). It is possible to remove almost completely the polishing grooves by an additional polishing with alumina solution (Struers FF alumina suspension), but in this case the surface of titanium is markedly altered, exhibiting holes similar to corrosion pits.

The surface topography of such mechanically polished samples after the electropolishing process is shown in Fig. 1(b). The polishing grooves are no longer present (images have been taken up to 50×50 μm^2), and the surface is homogeneous down to the size of the grains. This is an indication that the condition of microsmoothing by the electropolishing is fulfilled.[12]

An attempt of producing flat surfaces by vacuum evaporation of Ti/mica is shown in Figs. 1(c) and 1(d). At low substrate temperature [570 K, Fig. 1(c)], the topography is granular and homogeneous with a grain size slightly higher than for electropolished titanium (comparison of these topographies has been published elsewhere[13]). When the mica is held at 770 K during the evaporation [Fig. 1(d)], the titanium film exhibits flat terraces [the black to white z scale is 15 nm for Fig. 1(c) and 6 nm for Fig. 1(d)]. This results from the epitaxial growth of Ti/mica at these temperatures. Similar terraces and temperature dependence are found on gold.[14] Obviously, in the case of titanium we cannot expect an atomically flat surface because of the formation of the oxide during air exposure.

The true three-dimensional imaging capabilities of the SFM enables it to make a fractal analysis of the surface topography.[15] This provides a convenient way to catch the homogeneity of the topography over a large range of scan dimensions. It has been shown[16] that measuring the fractal dimension by means of a single SFM image is very subjected to artifacts. The appropriate way is to measure the rms roughness σ as a function of the lateral scale L in a series of images. If a power law $\sigma\sim L^H$ is obeyed over a wide range of L, the surface is said to be self-affine with a scaling exponent H and a fractal dimension $D=3-H$. For large scan areas, the motion of the piezotube scanner follows a parabola which drastically affects the value of σ and yields an erroneous value for the fractal dimension. Therefore, the data are corrected after the acquisition by a second-order polynomial at each line scan. The plots of $\ln\sigma$ vs $\ln(L)$ are represented in Fig. 2 for electropolished Ti and evaporated Ti on mica at low substrate temperature. These correspond to surface topography of Fig. 1(b) and 1(c), respectively, both showing a granular structure. In the case of electropolished titanium, the surface can be considered self-affine for $\ln[L(\text{Å})]>9$ with $H=1/3$. The value of L which separates the fractal and the nonfractal regime is often referred to as the crossover: We found a value of 0.8 μm for electropolished titanium. For the opposite case, evaporated Ti/mica at low temperature, the value of $\ln(\sigma)$ is almost constant over the whole range of scan (0.5–120 μm) with a slight decrease from $L\approx10$ μm. The constant part is due to the flatness of the mica and simply says that the thickness of the Ti film is homogeneous. We attribute the decrease from $L\approx10$ μm to the fact that the image is formed by 256×256 pixels, so that each pixel represents an area of 40 nm^2. As can be shown on Fig. 1(c), this is more or less the size of the titanium grain. Therefore, from this scan size, each pixel averages over one or several grains and that is why the calculated rms value decreases.

B. Metal-oxide interface

One important issue in the metal-oxide system is the sharpness of the interface or the presence of suboxides of a well-defined stoichiometry: This can condition the mechanical properties as well as corrosion properties of the material.[17] The metal-oxide interface can be probed by angular-dependent XPS measurement provided the surface is sufficiently flat and the oxide film sufficiently thin compared to the inelastic mean free path of the escaping electrons. For

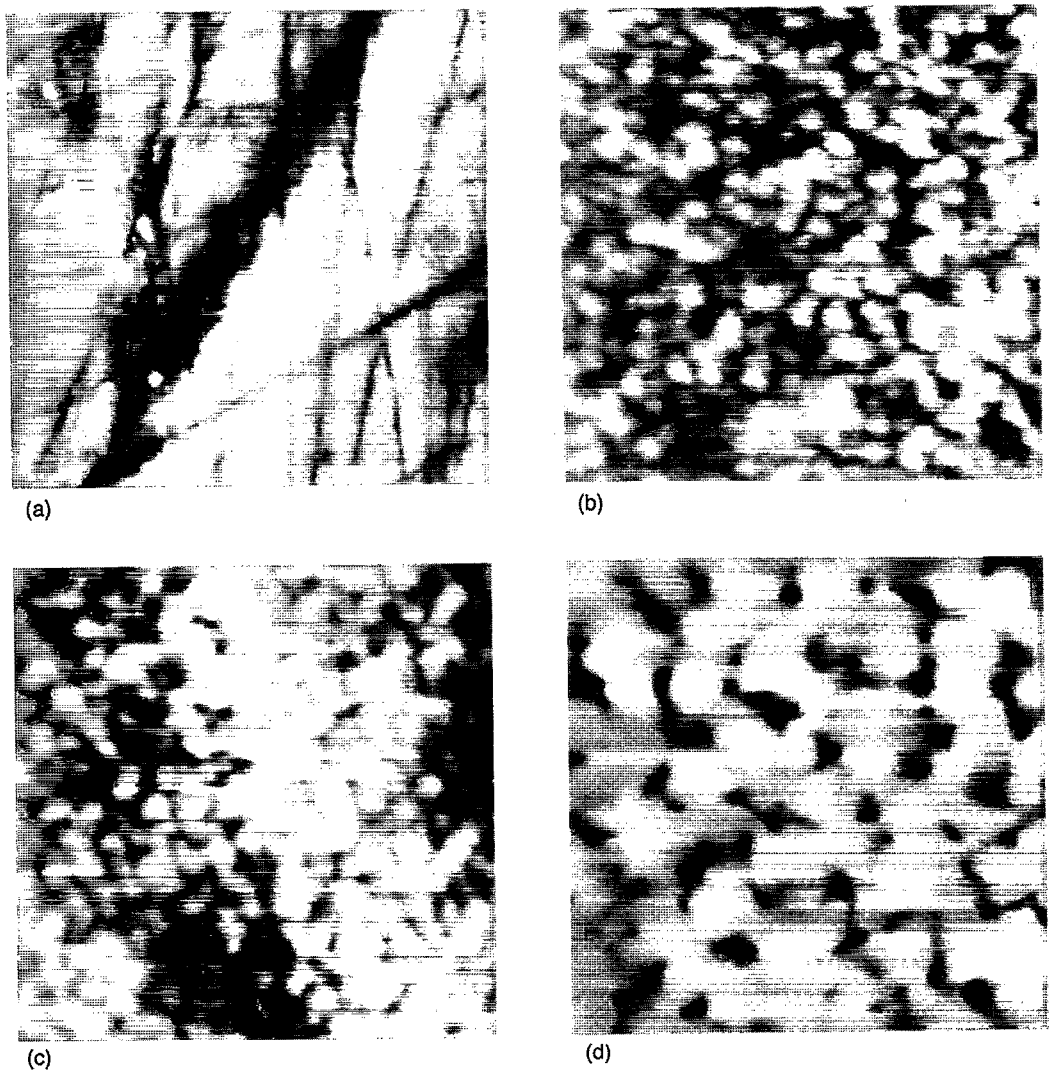

FIG. 1. Scanning force microscopy of various oxidized titanium surfaces: (a) mechanically polished [$5\times5\mu m^2$, vertical black-to-white (b/w) scale 100 nm]; (b) electropolished (0.86×0.86 μm^2, b/w scale 30 nm); (c) evaporated on mica at substrate temperature of 570 K (1×1 μm^2, b/w scale 15 nm); and (d) substrate temperature of 770 K ($1\times1\mu m^2$, b/w scale 6 nm).

this reason we have restricted our investigations to electropolished samples. However, even in this case, the topography is not flat enough to enable us an accurate determination of the suboxide thickness.

We have used monochromatized Mg $K\alpha$ radiation ($\hbar\omega = 1376$ eV) and a hemispherical energy analyzer (Surface Science Instrument SSX-100). XPS is well suited to the study of TiO_x since the chemical shifts of the Ti $2p$ peak are clearly resolvable for many oxides.[18] Relative to TiO_2, the chemical shift is -5.1 eV for metallic Ti, -3.5 eV for TiO, and -1.5 eV for Ti_2O_3.

Figure 3 shows the XPS Ti $2p$ spectra of electropolished titanium at three takeoff angles θ (the geometry is shown in the inset) which allow probing the valence states (oxidation state) with various sampling depths $d=\lambda\cos\theta$ (λ is the inelastic mean free path, which is of the order of 3–4 nm at these energies[19]). Therefore, the spectrum at $\theta=10°$ is mostly sensitive to the metal-oxide interface and the spectrum at $\theta=80°$ is the most surface sensitive. The peaks at 453, 459, and 464.5 eV on the $\theta=10°$ spectrum correspond to metallic Ti $2p_{3/2}$, TiO_2 $2p_{3/2}$, and TiO_2 $2p_{1/2}$, respectively. The stoechiometry at the surface ($\theta=80°$) is purely TiO_2, as expected. The presence of suboxide at the metal-oxide interface is revealed by the shoulder at 457 eV that is increasingly visible as the probing depth increases (θ is smaller). The arrow indicates the position of Ti $2p_{3/2}$ for the metal and therefore shows that the shoulder is not related to this valence state.

In order to establish what specific suboxide is present, we have deconvoluted the spectrum at $\theta=10°$ (Fig. 4). The following fitting procedure has been used: The energies between the splitting of Ti $2p_{3/2}$ and Ti $2p_{1/2}$ were imposed as constraints for each TiO_x species (with values of Ref. 20) and the position of the peaks and their widths were free parameters. We used only Gaussian curves to fit the data and the iteration routine tried to minimize the χ^2 test. In Fig. 4(a) the fit uses only the TiO_2 valence state of titanium whereas in Fig. 4(b) both TiO_2 and Ti_2O_3 valence states were taken into

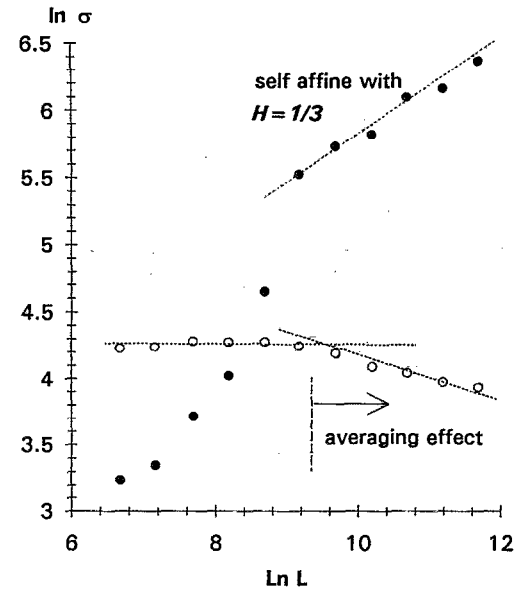

FIG. 2. The rms roughness (measured by SFM) vs the lateral scan dimension plotted on logarithmic scales for electropolished Ti (●) and evaporated Ti on mica at 570 K (○).

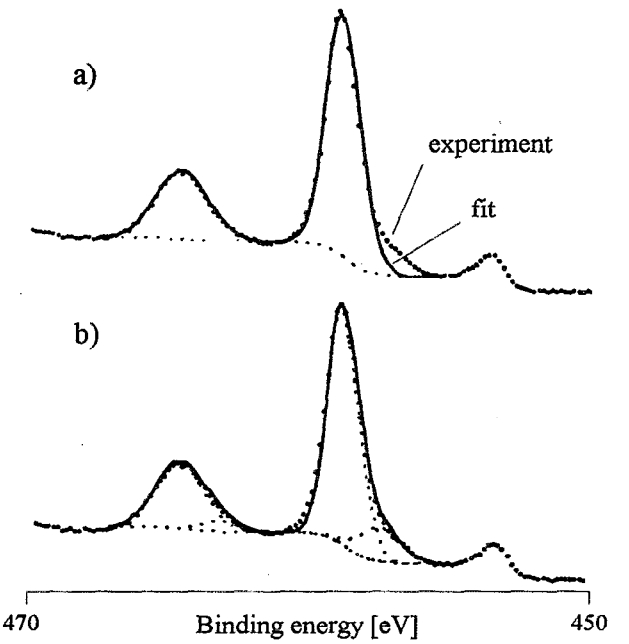

FIG. 4. Deconvolution of the Ti $2p$ spectrum of electropolished Ti at takeoff angle $\theta=10°$ showing the presence of the Ti_2O_3 valence state. Deconvolution using (a) TiO_2 only and (b) TiO_2 and Ti_2O_3.

account, demonstrating the presence of Ti_2O_3 at the metal-oxide interface. The accurate thickness of the Ti_2O_3 layer cannot be extracted with standard procedure of depth profile computing (such as the one described in Ref. 21) because this layer is too thin. Therefore, we conclude that the Ti_2O_3 layer is an interfacial layer of an estimated thickness of one or two atomic layers.

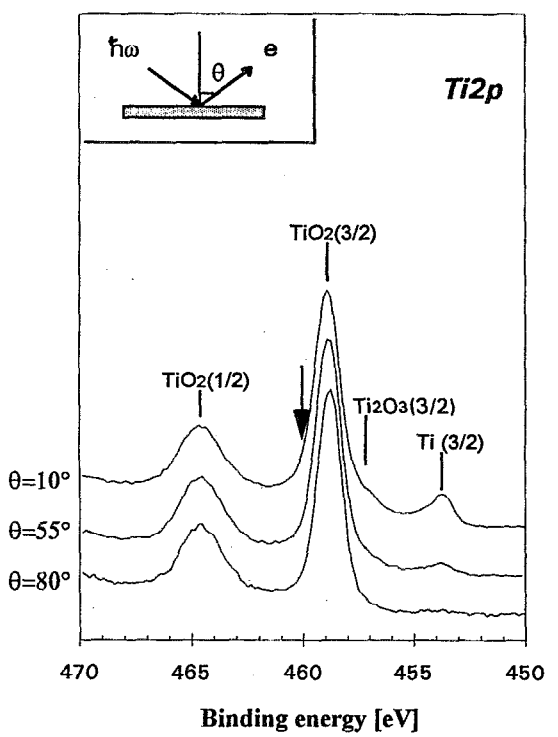

FIG. 3. Ti $2p$ XPS spectrum of electropolished titanium measured at various takeoff angles θ: (a) $\theta=10°$; (b) $\theta=55°$; (c) $\theta=80°$. The arrow indicates the position of metallic Ti $2p_{1/2}$.

C. XRD

As mentioned in Sec. I, the native oxide of titanium we are interested in is typically 5 nm thick which is not enough for normal XRD study. Unfortunately, most previous structural characterizations have been performed on thick films and mainly on TiO_2-deposited on substrates other than titanium.[4–8] To investigate to what extent we can easily change the structural properties of TiO_2 films on titanium, we have chosen to study the structure of thermally grown oxides. Furthermore, this preparation is close enough to be adopted as a model for the native oxide.

Our main purpose was to follow by XRD the dependence of the oxide structure on both the oxidation temperature and the crystallization state of the underlying metallic titanium. We have used an x-ray diffractometer (Siemens 5000) in the θ-2θ configuration with Cu $K\alpha$ radiation ($\lambda=1.506$ Å) and an acquisition time of 100 min.

We first present the results on the structure of the metallic titanium films. In Figs. 5(a) and 5(b) are shown the θ-2θ x-ray spectra of titanium evaporated on mica at a substrate temperature of 570 and 770 K, respectively. Since the thickness of the film is only 150 nm, the most prominent peaks are those of the underlying mica. The cleavage plane of mica is perpendicular to the c axis, and therefore we expect to see the (003) reflection (unit cell with $c=29.988$ Å) at the first and higher orders, and this is indeed the case. The large peak at $2\theta=38°$ observed in the sample evaporated at a substrate temperature of 770 K corresponds to the Ti(002) reflection, as expected since the (001) reflection has a zero structure factor. In the sample evaporated at a substrate temperature of

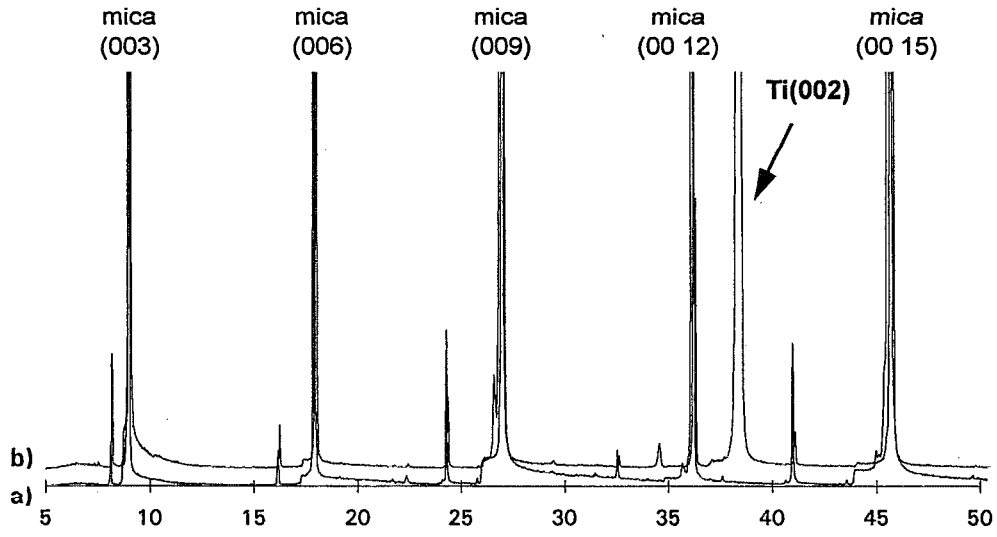

FIG. 5. XRD spectra of titanium films evaporated on mica at (a) $T=570$ K and (b) 770 K.

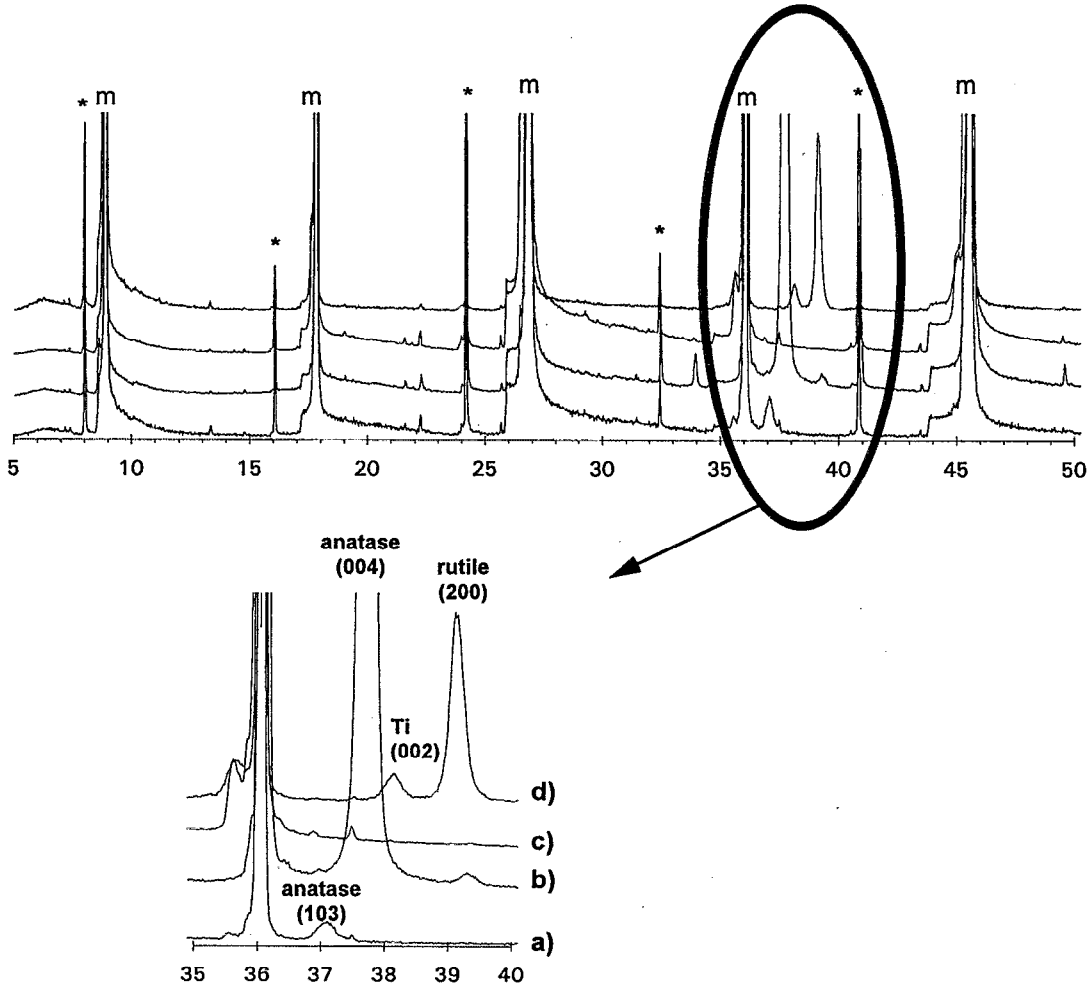

FIG. 6. XRD spectra of TiO_2 films thermally grown: (a) at 770 K on weakly crystallized Ti; (b) at 770 K on highly crystallized Ti; (c) at 970 K on weakly crystallized Ti; and (d) at 970 K on highly crystallized Ti.

TABLE I. XRD results on evaporated Ti and TiO_2 thermal oxides.

Mica temperature during Ti evaporation (K)	Crystallization of the metallic film	Dry oxidation temperature (K)	Crystallization of the TiO_2 oxide
570	none	770	weak anatase (103)
		970	strong anatase (004)
770	[highly Ti(0001) oriented]	770	none
		970	strong rutile (200)

570 K, the (002) reflection is absent, and no other titanium-related peaks are detected. Thus, the substrate temperature has a drastic effect illustrated by both the x-ray spectra and the SFM images: At 570 K the metallic film is weakly crystallized [on many of the films we have prepared, a small Ti(002) component is detectable] and has a granular surface topography [Fig. 1(c)] while at 770 K the film is strongly oriented along the c axis and the topography lets flat terraces appear [Fig. 1(d)].

Thermal oxides have been grown by heating these titanium films in oxygen containing atmosphere (see Sec. II) and we have looked at the influence on the phase and the orientation of the oxide of both the oxidation temperature and the crystallinity of the titanium films. XRD spectra of samples oxidized at 770 K are shown in Figs. 6(a) and 6(b) (for weakly and highly crystalline metallic film respectively) and at 970 K in Figs. 6(c) and 6(d) (again for weakly and highly crystalline metallic film, respectively). The peaks labeled "m" refer to the mica and "*" to their satellites. The other peaks are identified on the lower part of the figure. The differences between the various obtained thermal oxides are striking and described in the following.

At 770 K oxidation temperature of the initially highly crystallized Ti film a huge anatase (004) peak is observed with a small rutile component, while on the initially weakly crystallized Ti film, only a weak anatase phase is observed oriented along (103). Sputtered TiO_2 films on glass at 770 K also show a preferential growth along the (004) direction,[22] similar to our oxides on crystallized metallic Ti. However, we note that the lack of crystallinity of the titanium is sufficient to prevent the formation of a crystallized thermal oxide.

The results of thermal oxidation at 970 K are shown in Figs. 6(c) and 6(d) and again lead to completely different oxides. The highly crystallized film produced a TiO_2 rutile oriented along the (200) direction and not oriented along the (110) or (101) as is often the case for sputter-deposited rutile films at these temperatures.[23] Furthermore, this film still has a metallic Ti(002) component after oxidation (in contrast to oxidation at 770 K), which shows that the rutile formation at high temperature is limited in thickness or slower than the anatase formation at lower temperature. We then observe a faster oxide formation at lower temperature, which is not excluded *a priori* since we are dealing with distinct phases and since the enthalpy of formation of the rutile phase is slightly higher than the one of the anatase phase.[24] The weakly crystallized Ti film led to an almost completely amorphous oxide film, in particular, no rutile phase was detected. All the XRD results are summarized in Table I.

In conclusion, the structural difference of thermally grown oxide on highly crystallized Ti corresponds reasonably to the anatase to rutile transition observed on sputter-deposited TiO_2 films (although with different orientations), while only amorphous oxide films are formed on initially poorly crystallized Ti, even at high temperature.

D. EELS

In an EELS experiment we observe inelastic processes due to plasmons excitation and interband transitions in the 0–100 eV range below the elastic peak. We have acquired EELS spectra on polished and electropolished titanium, as well as on TiO_2(110)-rutile single crystal as a reference. The motivation of these measurements is the following. The native oxides resulting from electropolishing or mechanical polishing are formed very fast, at room temperature and the total thickness of the oxide is very small so that the formation of crystallites is unlikely. However, even if the native oxide is amorphous, we can ask whether the local atomic environment is similar to that of the crystalline phases of TiO_2. In the crystalline forms of TiO_2, the titanium atom binds in an octahedral configuration to six oxygen atoms. The molecular orbitals of such a $(TiO_6)^{8-}$ can be calculated and give the possible transitions that can be observed by EELS.[25] Therefore, a direct comparison of the EELS spectra of TiO_2 rutile and the native oxides gives an insight into the local environment of the titanium atoms in the native oxides.

We used a cylindrical mirror analyzer spectrometer with a coaxial electron gun (Varian). Maximum surface sensitivity is obtained at the lowest incident primary energy, which was set in our case to 150 eV (the beam is not stable at lower energy). The EELS spectra were recorded in the derivative mode dN/dE using a lock-in amplifier (1 $V_{p\text{-}p}$ sine wave modulation at 17 kHz) and the time acquisition was 8 min.

Figure 7 shows the EELS spectra at $E_i = 150$ eV for polished titanium, electropolished titanium, and TiO_2(110) rutile. The precise assignment of each of the structures can be readily done,[25] but is not of interest for the present purpose. What is immediately apparent on the spectra is that most of the features on the TiO_2 rutile are also present on the native oxides. The absence of the loss at 10 eV for electropolished titanium represents the main difference between the samples. According to Ref. 26, the loss at 10 eV is a signature of the Ti^{4+} species since it is not present on Ti_2O_3 single crystal. Therefore, electropolished titanium seems to have more Ti^{3+} defects trapped in its oxide: actually, this is consistent with the XPS angular-dependent measurements

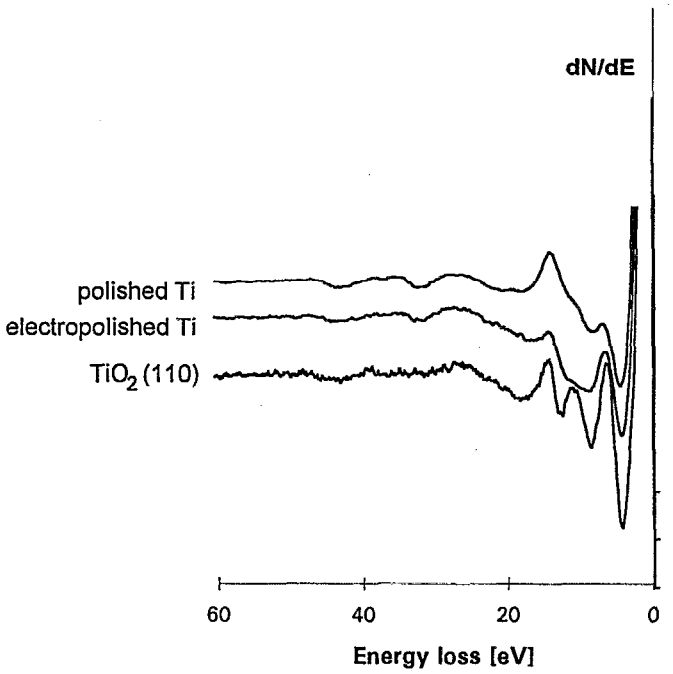

FIG. 7. EELS spectra of native titanium oxides compared to TiO_2(110) rutile.

(Sec. III B) which show the presence of the Ti_2O_3 layer at the metal-oxide interface. Therefore, since the main discrepancy between the crystallized TiO_2 and the native oxides can be explained, we can conclude that the local environment near the surface of the native oxides is similar to the one of crystallized TiO_2.

IV. CONCLUSIONS

Vacuum evaporation of titanium on mica at 770 K has been found to be a much more effective way to produce very flat homogeneous Ti films than any kind of polishing process. Highly oriented thermal oxides of titanium can be grown provided the underlying titanium is crystallized. The orientations of the thermal oxides differ from those obtained by sputtering TiO_2 films at the same temperature. Finally, even if the native titanium oxides can be strongly suspected to be amorphous, the local octahedral environment of the O atoms around Ti atoms is preserved in such oxides.

ACKNOWLEDGMENTS

The XPS measurements have been performed during a stay by one of us (M.J.) at the NESAC/BIO (University of Washington, Seattle) and Professor B. D. Ratner and his collaborators are acknowledged. We also thank L. Miéville for his help and Ch. Lüthi for technical assistance. This project was supported by the Swiss National Fund for Scientific Research, ITI Foundation, the Schmidheiny Foundation, and CERS.

[1] P. Tengvall and I. Lundström, Clin. Mater. **9**, 115 (1992).
[2] H. Sankur and W. Gunnig, J. Appl. Phys. **66**, 4747 (1989).
[3] A. Fujishima and K. Honda, Nature **238**, 37 (1972).
[4] M. Gasgnier, F. Lagnel, B. Poumellec, and J. F. Marucco, Thin Solid Films **187**, 25 (1990).
L. Meng, M. Andritschky, and M. P. dos Santos, Appl. Surf. Sci. **65/66**, 235 (1993).
[5] L. M. Williams and D. W. Hess, J. Vac. Sci. Technol. A **1**, 1810 (1983).
[6] L. S. Hsu, R. Rujkorakarn, J. R. Sites, and C. Y. She, J. Appl. Phys. **59**, 3475 (1986).
[7] G. A. Battiston, R. Gerbasi, M. Porchia, and A. Marigo, Thin Solid Films **239**, 186 (1994).
[8] L. S. Hsu, R. Solanki, G. J. Collins, and C. Y. She, Appl. Phys. Lett. **45**, 1065 (1984).
[9] T. Albrektsson, P. I. Branemark, H.-A. Hansson, B. Kasemo, K. Larsson, I. Lundström, D. H. McQueen, and R. Skalak, Ann. Biomed. Eng. **11**, 1 (1983).
[10] M. Jobin, M. Taborelli, and P. Descouts, Appl. Surf. Sci. **72**, 363 (1993).
[11] E. Grünbaum and R. Schwarz, J. Appl. Phys. **40**, 3364 (1969).
[12] For a discussion of micro- and macrosmoothing of electropolishing, see: D. Landolt, Electrochem. Acta **32**, 1 (1987).
[13] M. Jobin, M. Taborelli, R. Emch, F. Zenhausern, and P. Descouts, Ultramicroscopy **42-44**, 637 (1992).
[14] C. A. Lang, M. M. Dovek, J. Nogami, and C. F. Quate, Surf. Sci. **224**, L947 (1989).
[15] R. C. Salvarezza, L. Vázquez, P. Herrasti, P. Ocón, J. M. Vara, and A. J. Arvia, Europhys. Lett. **20**, 727 (1992).
J. Krim, I. Heyvaert, C. van Haesendonck, and Y. Bruynseraede, Phys. Rev. Lett. **70**, 57 (1993).
[16] J. M. Williams and T. P. Beebe, J. Phys. Chem. **97**, 6249 (1993).
[17] N. Sato, Corrosion Sci. **31**, 1 (1990).
[18] A. F. Carley, P. R. Chalker, J. C. Rivière, and M. W. Roberts, J. Chem. Soc. Faraday Trans. **83**, 351 (1987).
[19] M. P. Seah and W. A. Densch, Surf. Interf. Anal. **1**, 2 (1979).
[20] *Handbook for X-ray Photoemission Spectroscopy* (Perkin-Elmer, Physical Electronics Division, Minneapolis, MN, 1978).
[21] B. J. Tayler, D. G. Castner, and B. D. Ratner, Surf. Interf. Anal. **14**, 443 (1989).
[22] L. Meng, M. Andritschky, and M. P. dos Santos, Appl. Surf. Sci. **65-66**, 235 (1993). The amorphous nature of glass indicates that the formation of (004) anatase TiO_2 is not induced by the substrate.
[23] J. A. Eastmann, J. Appl. Phys. **75**, 770 (1994).
[24] G. V. Samsonov, *The Oxide Handbook* (Plenum, New York, 1982), p. 23.
[25] For a discussion of the features on TiO_2 rutile, see M. Mohamed, H. Sadeghi, and V. E. Heinrich, Phys. Rev. B **37**, 8417 (1988).
[26] V. E. Henrich, G. Dresselhaus, and H. J. Zieger, Phys. Rev. Lett. **36**, 1335 (1976).